Eurographics Workshop on Visual Computing for Biology and Medicine (2018)
I. Hotz, B. Kozlikova, and P.-P. Vazquez (Editors)

Short Paper

A Framework for Visual Comparison of 4D PC-MRI Aortic Blood Flow Data

B. Behrendt[1] and S. Ebel[2] and M. Gutberlet[2] and B. Preim[1]

[1]Dept. of Simulation and Graphics, University of Magdeburg, Germany
[2]Dept. of Diagnostic and Interventional Radiology, Herzzentrum Leipzig, Germany

Abstract

Four-dimensional phase-contrast magnetic resonance imaging (4D PC-MRI) allows for the non-invasive acquisition of in-vivo blood flow, producing a patient-specific blood flow model in selected vascular structures, e.g. the aorta. In the past, many specialized techniques for the visualization and exploration of such datasets have been developed, yet a tool for the visual comparison of multiple datasets is missing. Due to the complexity of the underlying data, a simple side-by-side comparison of two datasets using traditional visualization techniques can only yield coarse results.

In this paper, we present a toolkit that allows for an efficient and robust registration of different 4D PC-MRI datasets and offers a variety of both qualitative and quantitative comparison techniques. Differences in the segmentation and time frame can be amended semi-automatically using landmarks on the vessel centerline and flow curve of the datasets. A set of measures quantifying the difference between the datasets, such as the flow jet displacement or flow angle and velocity difference, is automatically computed. To support the orientation in the spatio-temporal domain of the flow dataset, we provide bulls-eye plots that highlight potentially interesting regions. In an evaluation with three experienced radiologists, we confirmed the usefulness of our technique. With our application, they were able to discover previously unnoticed artifacts occurring in a dataset acquired with an experimental MRI sequence.

CCS Concepts

• ***Human-centered computing*** → ***Visualization toolkits;*** *Information visualization;*

1. Introduction

Four-dimensional phase-contrast magnetic resonance imaging (4D PC-MRI) allows the acquisition of in-vivo time-resolved measurements of blood flow in 3D. These measurements can provide valuable information for physicians about hemodynamics associated with specific cardiovascular pathologies, such as the Marfan syndrome or bicuspid aortic valves [vBB*17, BMB*12]. 4D PC-MRI can be applied to a variety of different vascular structures, including the left and right ventricle and even various neurovascular regions [SAG*14]. In this paper, we will focus on aortic blood flow, which is one of the primary application domains for 4D PC-MRI measurements.

A common way to extract quantitative information from 4D PC-MRI data is the placement of measuring planes, which are commonly used to obtain measures such as stroke volume and regurgitation fractions [KPG*16b]. However, these planes can be arbitrarily placed, so the comparability of measures between different datasets is limited. The ability to compare and contrast multiple datasets is key to gain new insights about the inter-relation between changes in blood flow and vessel morphology. A common way to compare 4D PC-MRI datasets is to extract and contrast images or quantitative measures of visualizations from each dataset. However, this approach not only requires the user to know what specific type of differences he is looking for, but it also bears the risk of overlooking possibly valuable details.

The explorative approach to comparing 4D PC-MRI data we present in this paper gives the user a flexible tool for the analysis of multiple 4D PC-MRI datasets. In addition to exploring singular datasets, the analysis of differences and similarities between multiple datasets can lead to further insights, regarding not only the specific characteristics of certain pathologies, but also the influences of data acquisition and reconstruction techniques.

2. Related Work

The comparison of complex information is a key part of data analysis. Although there exist a set of general techniques, such as juxtaposition and explicit encoding, each specific application requires a specialized solution to allow for effective comparisons [GAW*11]. Various methods have been explicitly developed for the explorative visualization of medical flow data [OJMN*18]. So far, visual comparisons of unsteady medical flow data were achieved using image-level techniques based on strong abstractions that typically repre-

DOI: 10.2312/vcbm.20181236

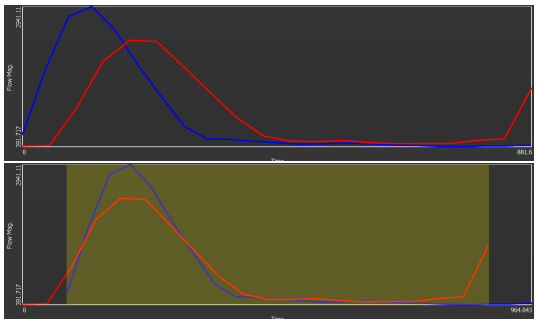

Figure 1: *Initial (top) and registered (bottom) flow curves of two datasets with overlapping time steps marked in yellow.*

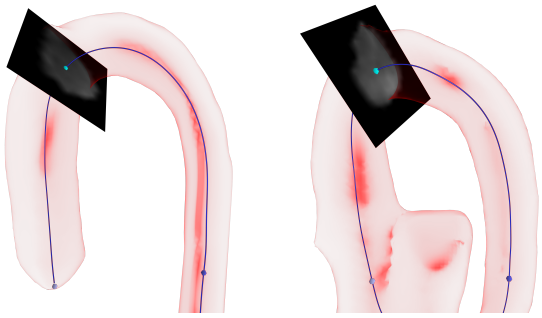

Figure 2: *Two datasets with a normalized centerline area between two markers.*

sent only some flow features. Van Pelt et al. developed a framework encompassing multiple visualizations [vBB*10]. They use illustrative techniques, such as contour rendering, to focus the flow visualization on relevant aspects. These techniques include the use of measuring planes to directly visualize the underlying flow field. The overall flow structures, such as vortices or branching flow, can also be represented using pathlines.

Köhler et al. developed a more abstract representation of vortex flow in cardiac vessels for the purpose of comparing multiple datasets by using circular bulls-eye plots [KMP*15]. The temporal position of a vortex is mapped to the angle, the position on the centerline to the distance from the plot center and the vorticity is mapped to color. The main goal of this visualization is to enable the physician to quickly distinguish between pathological and healthy flow structures. Due to the high level of abstraction, this method does not enable a more in-depth comparison between datasets.

3. Data Acquisition and Preprocessing

The 4D PC-MRI datasets used in this paper were acquired using 1.5T or 3T MRI-machines from Siemens Healthcare and stored in the DICOM format. From these images, the vessel geometry as well as a four-dimensional velocity vector field used to integrate pathlines is extracted. They also contain the patient coordinate matrix, which represents a transformation matrix to translate voxel coordinates from the dataset into world coordinates, including both position and orientation of the patient.

After importing the DICOM images, the aorta needs to be segmented. Since 4D PC-MRI images commonly suffer from low contrast, the segmentation is performed on higher-contrast MRI anatomy images. This is done semi-automatically using interactive graph cuts [BJ01], where the user has to iteratively specify regions on the image as back- or foreground [KPG*16a]. From the segmentation, a surface mesh representing the vessel geometry is created using the Marching Cubes algorithm and smoothed by the *vtkWindowedSincPolyDataFilter* module from the Visualization Toolkit (VTK). Afterwards, the centerline is extracted from the vessel geometry using the Vascular Modeling Toolkit (VMTK).

Lastly, pathlines representing the blood flow are integrated from the velocity field using fourth-order Runge-Kutte (RK4) integration. For each point of the resulting pathlines, a relative pressure value is calculated using the iterative pressure Poisson equation solver presented by Tyszka et al. [TLAS00].

4. Workflow

In cooperation with our clinical partners, we developed a workflow concept for the explorative comparison of 4D PC-MRI aortic blood flow data. The tools our partners are currently using are focused primarily on the visualization of single datasets. They are, however, interested in finding systematic differences between multiple datasets that are part of an ongoing study. A core component of our concept is image-based comparison using the juxtaposition of visualizations. Additionally, we provide feature-based comparisons by calculating and visualizing differences in flow velocity, direction and flow jet position of both datasets.

This section presents the workflow for our toolset, starting with the registration steps necessary for comparing datasets. Since we display information directly related to one of the datasets as well as to comparative measures between the datasets, we employ color-coding to distinguish these types of visualizations (red for the first dataset, blue for the second). Comparative visualizations are generally marked white.

4.1. Registration

For meaningful comparisons, the heart cycles depicted in both datasets need to be matched with each other. While performing the temporal registration, both datasets are represented by their flow curves. They are generated by adding up the flow magnitude from all voxels inside the segmentation for each time step. The resulting curve clearly shows the systolic and diastolic phases of the heart cycle (Fig. 1, top). In this case, the red dataset includes more than a single heart cycle, as a second systolic phase begins at its end. The user can manually adjust the offsets by dragging the curve onto a new position (Fig. 1, bottom). Additionally, the user has the option to add a scaling parameter to the datasets time frame in order to account for different heart rates. Due to the low temporal resolution of the datasets, a pixel-perfect registration of both curves is usually not required.

The spatial registration consists of three tasks: Visual registration, centerline normalization and rotational alignment. The visual

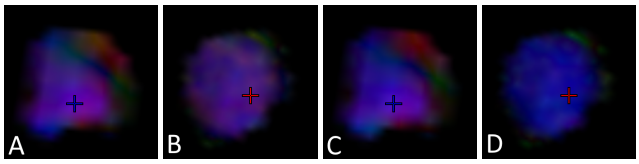

Figure 3: *Two planes sampled from two datasets (A,C / B,D) at the same anatomical position colorized by mapping the flow vectors to RGB colors. The left images use the data coordinate system, the right images use the local plane coordinate system.*

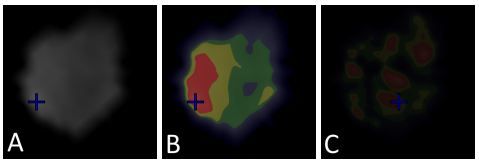

Figure 4: *Sampled plane with (B,C) and without (A) color overlay during the systolic (A,B) and diastolic (C) phase.*

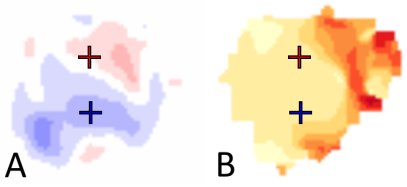

Figure 5: *2D comparative visualizations for flow velocity (A) and flow angle difference (B).*

registration can be performed mostly automatically by applying the patient matrix of each dataset to the surface and pathline models.

The centerline normalization is performed by placing landmarks. Initially, two markers are automatically placed at the beginning and end of the centerline, which can be independently moved along the centerlines of both datasets. They are used to crop the centerline, so that the remaining part covers the same anatomical areas in both datasets. In most cases, this is sufficient to normalize the centerline. However, in case of deformations of the vessel shape or the presence of bypasses, additional markers can be placed to achieve a satisfying normalization.

The rotational alignment needs to be performed manually by individually rotating each plane by up to 180°. The easiest way to find the correct angle is to move the planes to the supra-aortic vessel branches and rotate one of the planes until they correctly overlap in both planes.

4.2. 2D Visual Comparison

To extract 2D slices from the MRI data, multiple measuring planes can be created and moved along the vessel centerline (Fig. 2). The temporal position of a plane can be adjusted using a slider. By default, planes are squares with a side length of 4 cm, which is sufficient in most cases to cover the entire diameter of the aorta. If the aortic diameter strongly deviates from the norm at certain points, for example due to an aneurysm, the size of the individual planes can be manually adjusted.

Each plane is defined by their center position ($\vec{v_c}$) and three directional unit vectors ($\vec{v_x}$, $\vec{v_y}$ and $\vec{v_z}$). These vectors represent the local coordinate system of the plane, with the first two vectors spanning the plane and the last denoting its normal. We refer to the work of Köhler et al. for information about the calculation of these vectors [KPG*16b].

The sampled velocity vector $\vec{s}$ is visualized on the plane either by normalizing and directly mapping it onto RGB colors or by using a color scale. It is possible to toggle between the data coordinate system (where the X, Y and Z axis corresponds to the respective axes of the image grid) and the local plane coordinate system (where the coordinate system axes are represented by $\vec{v_x}$, $\vec{v_y}$ and $\vec{v_z}$). The rotated velocity vector $\vec{s'}$ is calculated using the dot product of the sampled vector with each of the local coordinate system axes.

With the plane coordinate system, it is easier to distinguish laminar flow (which primarily moves in the direction of the Z axis) from non-laminar flow (showing additional motion on the X and Y axis). This is exemplified in Figure 3. By switching to the plane coordinate system, it becomes clear that one plane (B, D) shows laminar flow (colored mostly blue due to being aligned with the Z axis), whereas the other one (A, C) does not. The flow jet position is shown in each plane using a cross (Fig. 3). It is calculated from the average of all pixel positions in the plane, weighted by velocity and normalized using the vessel diameter to reduce the influence of noise [SDW*15]. To better convey the shape of the flow, a color overlay highlighting the 50%, 75% and 90% quantile of the flow speed can be enabled (Fig. 4). The opacity of the color overlay is modulated with the ratio of the highest speed in the plane and the overall highest speed of the dataset to deemphasize slower diastolic flow, which is more susceptible to noise (Fig. 4, C).

In addition to showing data sampled directly from the flow fields, we also display two feature-based 2D comparative visualizations (Fig. 5). The first one shows differences in flow speed and is generated by subtracting the sampled flow speed of the second dataset from the first dataset (Fig. 5, A). In white areas, the flow speed is equal, whereas colored areas indicate that the respective dataset (red or blue) has faster flow at this position. The second comparative visualization shows differences in flow angles, with a color scale ranging from yellow (0° angle difference) to red (180° angle difference) (Fig. 5, B). The crosses highlighting the flow jet from both datasets are mirrored in the comparative visualizations as well.

The amount of freedom in positioning the measuring planes could easily cause details in the dataset to be overlooked, as the user would have to manually explore the entirety of the spatio-temporal domain of the dataset. Therefore, we added bulls-eye plots with an spatio-temporal encoding inspired by Köhler et al. [KMP*15] and familiar in cardiology as an overview visualization. Each point in these plots corresponds to a plane at a specific point in the spatio-temporal domain using polar coordinates. The distance from the center of the plot encodes the position on the centerline, the angle

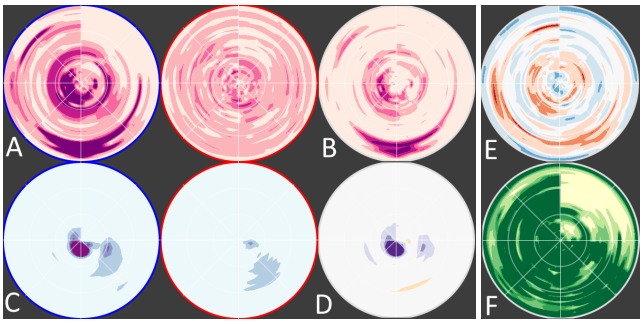

Figure 6: *Bulls-eye plots, showing individual (A) and comparative (B) flow jet displacement, individual (C) and comparative (D) regurgitation fraction, velocity (E) and angle comparison (F).*

encodes the time-point. Clicking on the plot will move the current measuring plane to the selected spatial and temporal position.

There is a total number of eight bulls-eye plots available (Fig. 6). The first six encode the flow jet displacement and regurgitation fraction (Fig. 6, A - D), which is an important clinical indicator for a heart valve disease. The first two plots of each type only show information from one of the datasets, therefore their outline is colored red and blue, respectively (Fig. 6, A and C). To calculate the flow jet displacement, the distance of the flow jet from the vessel centerline is computed for each plane and normalized with the vessel diameter. The last flow jet plot shows the distance between the flow jets in each dataset (Fig. 6, B). Similarly, the last regurgitation plot show a comparison of the regurgitation fractions of both datasets (Fig. 6, D). Two additional plots show a comparison between flow speed and average flow angle (Fig. 6, E and F).

To support orientation, a circular grid with eight radial lines is overlayed on top of the plot. All bulls-eye plots use discrete color scales to highlight regions with high or low values. Different types of information (e.g. flow jet, velocity, angle) are shown with different color scales to prevent confusion.

4.3. 3D Visual Comparison

The 3D visualization shows the surface model and pathlines of both datasets side-by-side using a synchronized camera, allowing for an image-based comparison. We consider the vascular surface to be a context object, therefore we use the Fresnel opacity presented by Gasteiger et al. to prevent occlusion with the inlying pathlines [GNKP10]. Parameters such as speed or pressure can be mapped onto the pathline color or opacity. To support orientation in the dataset, the selected planes are also visible in the 3D view. They can be individually hidden to prevent possible occlusion.

4.4. Implementation

Sampling from the velocity field is performed off-screen using a fragment shader in combination with multiple 2D textures bound to the framebuffer. The velocity field itself is stored as a set of 3D textures. Both the current and next time step are bound as active textures together with an interpolation value. Once for each texel of the 2D output texture, the fragment shader samples values from the velocity field and interpolates them according to the interpolation value.

Sampled data is written to three different textures. The first contains the raw flow data sampled from the flow field. The second and third textures are used for rendering and contain the data after the application of the color scale and the flow speed overlay, respectively. In both the 2D and 3D view, the user can switch between binding one of these textures, or both of them at the same time.

Once the user has finished the spatial and temporal registration, the flow jet and bulls-eye plots are generated. A number of planes is automatically placed spatially along the registered centerline with a distance of 1cm, which was chosen empirically as a trade-off between plane coverage and required computation time. For each plane, a set of values is calculated and stored in a single pixel of a two-dimensional image. These values include the flow jet position as a 2D vector, the flow jet displacement in relation to the centerline and the average flow velocity in the plane. This results in a square image where each pixel represents a single plane at a single point in time, covering the entire spatio-temporal domain. To display the flow jet or generate the bulls-eye plots, this image is then sampled using linear interpolation.

5. Evaluation

To evaluate our method, we performed an informal interview with three expert radiologists. They were shown a total of four aortic datasets available for a pair-wise comparison. Two were acquired from the same volunteer right after one another using different MRI sequences. Additionally, a dataset from a different volunteer as well as a patient dataset were used.

Overall, the radiologists found the ability to directly compare flow datasets useful. The amount and complexity of manual input required for the registration of the data was deemed acceptable. One of the physicians noted that if the DICOM data contained data about the heart rate during acquisition, this information could be used to normalize the flow velocity for both datasets in an optional pre-processing step. A point of critique was the lack of a way to restrict the spatio-temporal domain of the bulls-eye plots to certain phases of the heart beat or anatomical regions that the physicians were specifically interested in.

Two of the radiologists were especially interested in comparing data from the same patient, either at different time-points or using different sequences, to evaluate different MRI sequences or perform follow-up examinations. The third radiologist expressed interest in using our tool to support the extraction or standard values regarding blood flow in patients and healthy volunteers. The comparison of the two datasets acquired using different MRI sequences allowed the radiologists to detect artifacts in one of the datasets (Fig. 7). While one sequence shows primarily laminar flow, the same anatomical region contains a vortex when acquired using a different MRI sequence, which is clearly visible in the average flow angle bulls-eye plot (7, E). During the evaluation, the radiologists noticed a problem that affected the flow jet calculation in some of the datasets. Depending on the size of the measuring planes and the overall vessel geometry, a plane placed in the descending aorta may

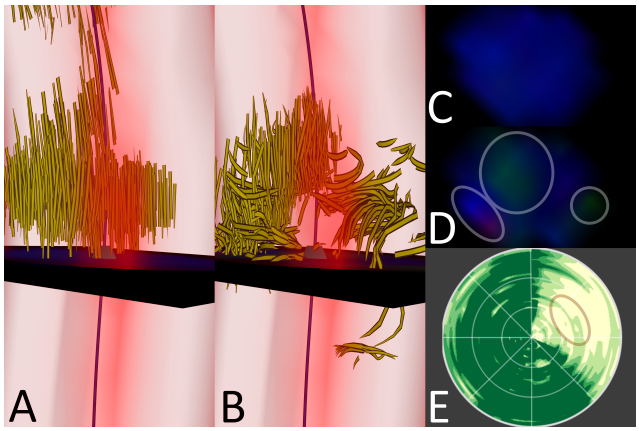

Figure 7: *Changes in flow representation (A,B) and average flow angle bulls-eye plot (E) due to deviations in the flow field (C,D) as a result of different MRI sequences.*

intersect with the left ventricle. This may impact the flow jet calculation, causing the bulls-eye plot to show a strong displacement that does not actually exist in the data.

6. Conclusion & Future Work

In this paper, we have presented a set of tools for the comparative exploration of two 4D PC-MRI datasets. An informal interview with three experienced radiologists indicated the usefulness of our approach. Although we focused on the examination of aortic blood flow, our methods should be applicable to other vessels such as the pulmonary artery with only minimal adjustments. However, the exploration of other structures, such as the left or right ventricle, would be more challenging due to the fact that we rely on the presence of a centerline to place measuring planes. Therefore, a different method of placing planes and performing a spatial MRI registration would need to be implemented. Additionally, a dynamic segmentation would be needed to account for the strong ventricular movement during the cardiac phases.

Currently, our application only allows comparisons between 4D PC-MRI datasets. In the future, we plan to add support for data from computational fluid dynamics (CFD) simulations. This would enable the user to explore the differences between measured and simulated flow in the same vessel. A key problem that would need to be solved is the handling of data with vastly different resolution and storage format. It may also be challenging to sample the high-resolution CFD data in real-time, requiring additional preprocessing steps to allow for an interactive frame-rate.

In addition to the visual exploration of the differences between two datasets, a tool to process a larger number of datasets would also be useful. This would support the systematic evaluation of a larger database of flow data. Such an approach requires a higher degree of automation regarding the registration as well as methods to automatically cluster the datasets based on their similarity and extract the systematic differences between the clusters.

Acknowledgments

We would like to give thanks to Prof. Matthias Grothoff and Dr. Katharina Fischbach for participating in our evaluation. Additional thanks go to Benjamin Köhler for the various fruitful discussions about the techniques used in this paper.

References

[BJ01] BOYKOV Y. Y., JOLLY M.-P.: Interactive graph cuts for optimal boundary & region segmentation of objects in N-D images. In *Eighth IEEE International Conference on Computer Vision* (2001), pp. 105–112. 2

[BMB*12] BARKER A. J., MARKL M., BÜRK J., LORENZ R., BOCK J., BAUER S., SCHULZ-MENGER J., VON KNOBELSDORFF-BRENKENHOFF F.: Bicuspid aortic valve is associated with altered wall shear stress in the ascending aorta. *Circulation. Cardiovascular imaging 5*, 4 (2012), 457–466. 1

[GAW*11] GLEICHER M., ALBERS D., WALKER R., JUSUFI I., HANSEN C. D., ROBERTS J. C.: Visual comparison for information visualization. *Information Visualization 10*, 4 (2011), 289–309. 1

[GNKP10] GASTEIGER R., NEUGEBAUER M., KUBISCH C., PREIM B.: Adapted Surface Visualization of Cerebral Aneurysms with Embedded Blood Flow Information. In *VCBM* (2010), pp. 25–32. 4

[KMP*15] KÖHLER B., MEUSCHKE M., PREIM U., FISCHBACH K., GUTBERLET M., PREIM B.: 2D Plot Visualization of Aortic Vortex Flow in Cardiac 4D PC-MRI Data. In *Bildverarbeitung für die Medizin 2015*, Handels H., Deserno T. M., Meinzer H.-P., Tolxdorff T., (Eds.), Informatik aktuell. Springer Berlin Heidelberg, Berlin, Heidelberg, 2015, pp. 257–262. 2, 3

[KPG*16a] KÖHLER B., PREIM U., GROTHOFF M., GUTBERLET M., FISCHBACH K., PREIM B.: Motion-aware stroke volume quantification in 4D PC-MRI data of the human aorta. *International journal of computer assisted radiology and surgery 11*, 2 (2016), 169–179. 2

[KPG*16b] KÖHLER B., PREIM U., GROTHOFF M., GUTBERLET M., FISCHBACH K., PREIM B.: Robust Cardiac Function Assessment in 4D PC-MRI Data of the Aorta and Pulmonary Artery. *Computer Graphics Forum 35*, 1 (2016), 32–43. 1, 3

[OJMN*18] OELTZE-JAFRA S., MEUSCHKE M., NEUGEBAUER M., SAALFELD S., LAWONN K., JANIGA G., HEGE H.-C., ZACHOW S., PREIM B.: Generation and Visual Exploration of Medical Flow Data: Survey, Research Trends and Future Challenges. *Computer Graphics Forum 40*, 4 (2018), 860. 1

[SAG*14] STANKOVIC Z., ALLEN B. D., GARCIA J., JARVIS K. B., MARKL M.: 4D flow imaging with MRI. *Cardiovascular diagnosis and therapy 4*, 2 (2014), 173–192. 1

[SDW*15] SIGOVAN M., DYVERFELDT P., WRENN J., TSENG E. E., SALONER D., HOPE M. D.: Extended 3D approach for quantification of abnormal ascending aortic flow. *Magnetic resonance imaging 33*, 5 (2015), 695–700. 3

[TLAS00] TYSZKA J. M., LAIDLAW D. H., ASA J. W., SILVERMAN J. M.: Three-dimensional, time-resolved (4D) relative pressure mapping using magnetic resonance imaging. *Journal of magnetic resonance imaging : JMRI 12*, 2 (2000), 321–329. 2

[vBB*10] VAN PELT R., BESCÓS J. O., BREEUWER M., CLOUGH R. E., GRÖLLER M. E., TER HAAR ROMENIJ B., VILANOVA A.: Exploration of 4D MRI Blood Flow using Stylistic Visualization. *IEEE transactions on visualization and computer graphics 16*, 6 (2010), 1339–1347. 2

[vBB*17] VAN DER PALEN R. L. F., BARKER A. J., BOLLACHE E., GARCIA J., ROSE M. J., VAN OOIJ P., YOUNG L. T., ROEST A. A. W., MARKL M., ROBINSON J. D., RIGSBY C. K.: Altered aortic 3D hemodynamics and geometry in pediatric Marfan syndrome patients. *Journal of Cardiovascular Magnetic Resonance 19*, 1 (2017), A164. 1